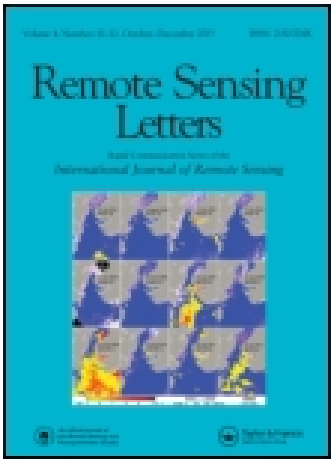

Remote Sensing Letters
Publication details, including instructions for authors and subscription information:
http://www.tandfonline.com/loi/trsl20

A comparison of Gaussian process regression, random forests and support vector regression for burn severity assessment in diseased forests

Carolynne Hultquist[a], Gang Chen[a] & Kaiguang Zhao[b]
[a] Department of Geography and Earth Sciences, University of North Carolina at Charlotte, Charlotte, North Carolina, USA
[b] Ohio Agricultural and Research Development Center, School of Environment and Natural Resources, The Ohio State University, Wooster, Ohio, USA
Published online: 29 Sep 2014.

To cite this article: Carolynne Hultquist, Gang Chen & Kaiguang Zhao (2014) A comparison of Gaussian process regression, random forests and support vector regression for burn severity assessment in diseased forests, Remote Sensing Letters, 5:8, 723-732, DOI: 10.1080/2150704X.2014.963733

To link to this article: http://dx.doi.org/10.1080/2150704X.2014.963733

Remote Sensing Letters, 2014
Vol. 5, No. 8, 723–732, http://dx.doi.org/10.1080/2150704X.2014.963733

Taylor & Francis
Taylor & Francis Group

A comparison of Gaussian process regression, random forests and support vector regression for burn severity assessment in diseased forests

Carolynne Hultquist[a], Gang Chen[a]*, and Kaiguang Zhao[b]

[a]*Department of Geography and Earth Sciences, University of North Carolina at Charlotte, Charlotte, North Carolina, USA;* [b]*Ohio Agricultural and Research Development Center, School of Environment and Natural Resources, The Ohio State University, Wooster, Ohio, USA*

(*Received 20 May 2014; accepted 2 September 2014*)

Remote sensing has been widely adopted to map post-fire burn severity over large forested areas. Statistical regression based on linear or simple non-linear assumptions is typically used to link post-fire forest reflectance with the degree of burn severity. However, this linkage becomes complicated if forests experienced severe mortality caused by pre-fire disease or insect outbreaks, which is likely to occur more frequently as a result of rapid climate change. In an effort to improve the understanding of the relationship between forest reflectance and fire-disease disturbances, this study explored the efficacy of three machine learning techniques, that is, Gaussian process regression (GPR), random forests (RF) and support vector regression (SVR), within a geographic object-based image analysis (GEOBIA) framework to assess burn severity in a forest subject to pre-fire disease epidemics. MASTER [MODIS (Moderate Resolution Imaging Spectroradiometer)/ASTER (Advanced Spaceborne Thermal Emission and Reflection Radiometer)] airborne sensor was applied to collect relatively high spatial (4 m) and high spectral (50 bands) resolution reflectance data. Results show that RF, SVR and GPR models outperformed conventional multiple regression by 48%, 29% and 27%, respectively. Compared to SVR and GPR, RF not only achieved better performance in burn severity assessment, but also demonstrated lower sensitivity to the application of different combinations of remote sensing variables. In addition to Normalized Burn Ratio (NBR), this study further revealed the importance of image-texture (representing spectral variability within and between neighbourhood forest patches) in burn severity mapping over diseased forests.

1. Introduction

High-profile wildfires have led to significant impacts on climate and terrestrial ecosystems (Malamud, Millington, and Perry 2005). In a forest environment, fire can affect vegetation structure, plant species diversity and biomass carbon stocks across spatial scales from the individual tree to the landscape level (Keith, Mackey, and Lindenmayer 2009). As a measure of post-fire effects on local and regional environments, burn severity becomes a standardized index facilitating assessments of fire-induced vegetation consumption, mortality and recovery in forest management (Lentile et al. 2006). Field mensuration to map burn severity is subject to logistical challenges and lacks a substantial amount of spatial details, because unburned and lightly burned patches often intersperse among severely burned patches due to the variability in landscape patterns and microclimates (Cocke,

*Corresponding author. Email: gang.chen@uncc.edu

Fule, and Crouse 2005). Remote sensing, which provides a synoptic view of large burned landscapes using spaceborne or airborne sensors, has been widely adopted to map the post-fire ecological effects in forests (Lentile et al. 2006).

The major challenge for remotely assessing burn severity is that imagery integrates changes from all parts of the trees, including those on the ground and in the canopies (White et al. 1996). In recent years, researchers have further found that diseases and insects are likely to occur in fire-prone forest landscapes (Jenkins et al. 2008; Metz et al. 2011; Harvey et al. 2013). This means that wildfires may interact with both healthy and infested forests during the same fire events. Consequently, the degree of burn severity, the structure of trees and the stage of infestation together could add high complexity to analyse the spectral reflectance from burned and infested landscapes. The conventional statistical regression or classification based on linear or simple non-linear assumptions to link post-fire forest reflectance with field measurements may therefore have difficulties to meet burn severity mapping requirements, often leading to large errors (De Santis and Chuvieco 2007). Recent machine learning techniques (e.g., Gaussian process regression (GPR), random forests (RF) and support vector regression (SVR)) offer some promising alternatives, because they have proven effective to account for complex non-linear relationships between variables with superior performances demonstrated in a preponderance of comparative research for forest applications (Chen and Hay 2011; Zhao et al. 2011). They have also revealed high capacity to tackle the data noise and high-dimensional problems, possibly introduced by the utilization of advanced remote sensing data sets featuring high spatial and/or high spectral resolution (Zhao et al. 2011; Dalponte, Bruzzone, and Gianelle 2012). Despite the advantages, machine learning was rarely used in burn severity assessment, especially in forests suffering from fire-disease disturbances.

The main objective of this study is to explore the efficacy of three machine learning techniques, that is, GPR, RF and SVR, to assess burn severity in a forest that experienced pre-fire disease outbreaks. To do so, we apply MASTER [MODIS (Moderate Resolution Imaging Spectroradiometer)/ASTER (Advanced Spaceborne Thermal Emission and Reflection Radiometer)] airborne imagery (see sensor details in Hook et al. 2001) with relatively high spatial (4 m) and high spectral (50 bands) resolution to examine the utility of machine learning in analysing advanced remote sensing data sets, and compare the burn severity modelling results of machine learning with those of typical multiple regression.

2. Data collection

2.1. Study area

Our study site (centred at: 36°15′N, 121°43′W) is located in the Big Sur California ecoregion, covering an area of 28,383 ha (Figure 1). It features a Mediterranean-type climate with a rugged landscape that is dissected by steep slopes and drainages with elevations ranging from sea level to 1571 m within 5 km of the coast (Meentemeyer et al. 2008). Major forest types in the area include mixed coniferous forests, mixed oak woodlands and redwood–tanoak dominant forests. Since the mid-1990s, a non-native pathogen *Phytophthora ramorum* causing the disease sudden oak death (SOD) has led to substantial mortality in the region. In 2008, major wildfires occurred for the first time in forests affected by SOD. The largest fire, Basin Complex Fire, burned over 95,000 ha including our study area.

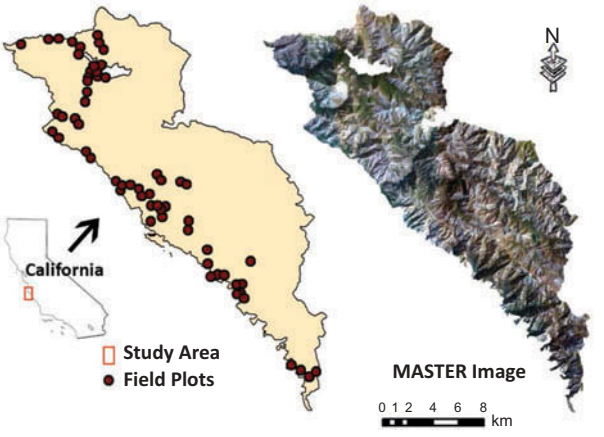

Figure 1. Study area located in the Big Sur ecoregion on the western flank of the Santa Lucia Mountains in California. The MASTER preprocessed image mosaic is from a colour composite using bands 5 (red), 3 (green) and 1 (blue).

2.2. Field data

A network of long-term SOD-monitoring plots (500 m^2 each) in Big Sur was established in 2006 and 2007 to understand the responses of forest communities (e.g., host mortality) to the invasion of SOD. In September and October 2008, immediately following the containment of the Basin Complex Fire, a total of 61 plots were revisited to assess burn severity using Composite Burn Index (CBI) (Key and Benson 2006). In this study, the average CBI representing an overall burn effect in each plot was used.

2.3. Remote sensing data

The MASTER (MODIS/ASTER) airborne simulator was applied to collect 12 image scenes covering the area on 26 August 2008 (approximately 1 month after the fire perimeter was contained). All images had 50 bands including the visible and near-infrared (VNIR) and short-wave infrared (SWIR) (bands 1–25), the mid infrared (MIR: bands 26–40) and the thermal infrared (TIR: bands 41–50) regions. The spatial resolution of the imagery was 4 m, and the data were radiometrically and geometrically calibrated at the Level 1B before delivered by the vendor.

Prior to burn severity modelling, the images were preprocessed using the following four steps: (1) minimizing the view-angle brightness gradient, (2) image mosaicking, (3) radiometric correction and (4) topographic correction. Specifically, (1) the sun and sensor geometry influences the data quality with each image transect being relatively bright on one side and dark on the other side. To minimize this view-angle brightness gradient, we fit a quadratic curve to each column to simulate the changes in brightness across view angles and then applied a multiplicative compensation method to compensate each pixel (Kennedy, Cohen, and Takao 1997). (2) The 12 transects were then mosaicked in sequence using the overlapped area from one image to balance the data range of its neighbouring image. (3) The dark object subtraction algorithm was used to derive surface radiance (Chavez 1996) in the VNIR and SWIR region. No atmospheric correction was applied to the MIR region, as it is insensitive to the presence of most aerosols (Harris, Veraverbeke, and Hook 2011). In the TIR region, surface emissivity was extracted by separating from surface temperature using the emissivity

normalization technique developed by Kealy and Hook (1993). (4) A topographic correction was applied to normalize for different illumination conditions caused by topography using the C-correction method (Teillet, Guindon, and Goodenough 1982), with the preprocessed image mosaic shown in Figure 1.

3. Methodology

3.1. Object-based variable extraction

The MASER image mosaic was segmented using a geographic object-based image analysis (GEOBIA) approach to generate image objects at a relatively small tree patch level aiming to characterize heterogeneity in the burned and infested forests while reducing high spectral variation. To do this, eCognition Developer 8 (Trimble Navigation, Sunnyvale, California) was applied to generate image objects with an average size of 0.8 ha (Figure 2). All the variables used in the succeeding burn severity assessment were extracted from these objects and are considered as object-based variables.

The independent object-based variables were derived from MASTER imagery and categorized into three types: original spectral bands, image-texture and spectral indices. The 50 original spectral bands (hereafter: Spectral) was derived by averaging pixel values within image objects for the 50 MASTER bands. Image-texture was calculated for each of the spectral bands, comprising two types of texture variables, that is, internal texture (TXIT) and neighbourhood texture (GEOTEX). Specifically, TXIT represented the standard deviation within each object, while GEOTEX characterized the relationship between neighbourhood objects where standard deviation was calculated using the averaged pixel values from the centre object and its immediate neighbours (Chen et al. 2011). We have calculated several spectral indices, including Normalized Burn Ratio (NBR), Normalized Difference Vegetation Index (NDVI), SWIR–MIR Index (SMI), NIR–SWIR–Emissivity version 1 (NSEv1), which have been proven effective in previous burn severity studies covering a wide spectral range from VNIR–SWIR to TIR (Tucker 1979; Kaufman and

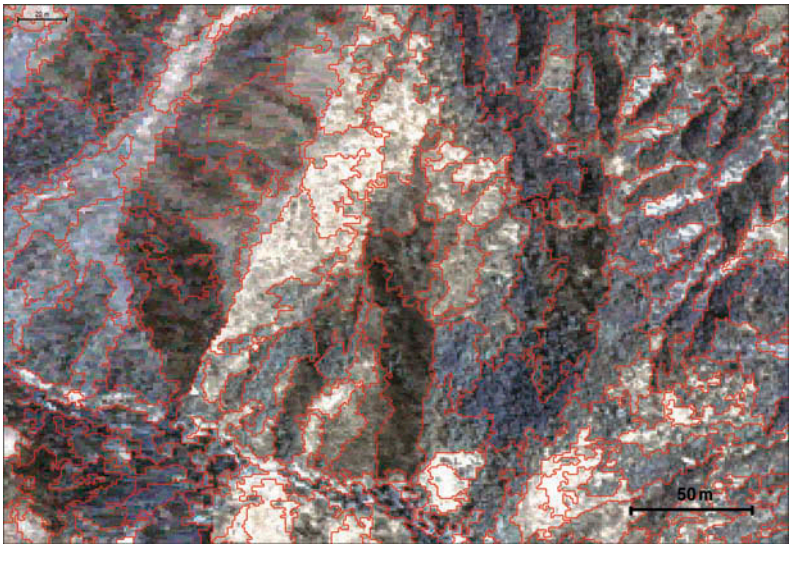

Figure 2. A sample area with red lines representing the boundaries of segments and white colour signifying the cover of post-fire white ash.

Remer 1994; Key and Benson 2006; Veraverbeke, Hook, and Hulley 2012). The MASTER bands used to calculate these indices are presented in the following equations:

$$\mathrm{NBR} = (\mathrm{NIR} - \mathrm{LSWIR})/(\mathrm{NIR} + \mathrm{LSWIR}) \quad (1)$$

$$\mathrm{NDVI} = (\mathrm{NIR} - \mathrm{Red})/(\mathrm{NIR} + \mathrm{Red}) \quad (2)$$

$$\mathrm{SMI} = (\mathrm{SSWIR} - \mathrm{MIR})/(\mathrm{SSWIR} + \mathrm{MIR}) \quad (3)$$

$$\mathrm{NSEv1} = ((\mathrm{NIR} - \mathrm{LSWIR})/(\mathrm{NIR} + \mathrm{LSWIR})) \times \mathrm{E} \quad (4)$$

where NIR is near infrared (reflectances from band 9), SSWIR is shorter short-wave infrared (reflectances from band 12), LSWIR is longer short-wave infrared (reflectances from band 24), MIR is mid infrared (reflectances from band 29) and E is emissivity (reflectances from band 43). Consequently, a total of 154 independent variables were extracted. The object-based dependent variable was calculated by overlaying field plots onto image objects and then assigning field-measured CBI values to the spatially corresponding objects.

A machine learning minimal-redundancy-maximal-relevance approach (mRMR) was applied to select a subset of independent object-based variables, which was based on the principle of minimizing similarity between each variable, and maximizing relevance with the target class of field-measured CBI (Peng, Long, and Ding 2005). To facilitate straightforward comparisons of burn severity assessment, mRMR was used to generate consistent input variables for all the four types of models (i.e., multiple regression and three machine learning models). This study selected the top eight variables (in order of predicting power) and evaluated the model sensitivity to the application of different number of independent variables from top one to top eight.

3.2. *Multiple regression*

A linear regression model was developed to link mRMR-selected MASTER variables with field-measured CBI at the 0.05 significance level. All the field plots were randomly divided into two groups, with half of the plots used as training data and the remainder for validation. Root-mean-squared errors (RMSEs) of CBI were calculated with the independent validation plots. The same data groups were further applied to train and validate the machine learning models presented in the following sections, and their RMSEs were used for cross-comparison among the models.

3.3. *Random forests (RF)*

RF are a highly versatile ensemble of decision trees that performs well for linear and non-linear prediction by finding a balance between bias and variance (Breiman 2001; Segal 2003). This ensemble learning method is known as 'bagging' as it grows trees in which successive trees do not depend on earlier trees. Each tree is independently determined using a bootstrap sample of the data set and a simple majority vote is taken for final prediction (Liaw and Wiener 2002). Use of RF requires specifying two standard parameters: the number of input variables randomly chosen at each split at each node (mtry) and the number of trees (ntree). After exploratory trials using training data, we found little variability in the results of our burn severity assessment and finally chose the mtry value of 3 and the ntree value of 100 as model parameters.

3.4. Support vector regression (SVR)

SVR, originating from statistical learning theory, provides the capability to handle highly non-linear problems even with noisy training (Vapnik 1998). SVM essentially transforms the non-linear regression problem into a linear one by using kernel functions to map the original input space into a new feature space with higher dimensions, with an ability to find unique global solutions that are not inhibited by multiple local minima (Cristianini and Shawe-Taylor 2000). This study applied a model type ε-SVR in the regression (ε: precision parameter) and RBF as the kernel function. In ε-SVR, an ε-insensitive loss function is used for tolerating small errors between the predicted and true values as long as the errors are less than ε; RBF often leads to better model performance than the other kernels (Chen and Hay 2011). A two-step grid-search technique suggested by Hsu, Chang, and Lin (2009) was used to tune three model parameters, including penalty parameter (C), ε and kernel parameter (γ).

3.5. Gaussian process regression (GPR)

Similar to SVR, GPR is another popular kernel-based machine learning method for non-linear regression problems (e.g., Zhao et al. 2011). GPR is typically formulated and interpreted in a Bayesian context (Rasmussen and Williams 2006). To infer an unknown functional relationship from a training data set, GPR first elicits a prior GPR to constrain the possible forms of the unknown function and then updates this prior in the light of training samples to generate a posterior GPR as the final functional model (Rasmussen and Williams 2006; Zhao, Popescu, and Zhang 2008). The learning of a GPR model also needs to specify some parameters related to the covariance or kernel functions (also known as hyper-parameters). The hyper-parameters to be tuned for a RBF kernel include magnitude, characteristic length and noise variance, roughly corresponding to the C, γ and ε parameters of SVR (Pasolli, Melgani, and Blanzieri 2010). And the maximum-likelihood-II method (aka empirical Bayes or evidence approximation) was applied for parameter tuning in this study (Bishop 2006).

4. Results and discussion

4.1. Model sensitivity to variable selection

The application of the mRMR feature selection algorithm resulted in a list of object-based variables. The top eight selected variables, as ranked in terms of predictive power, were TXIT (band 14), GEOTEXT (band 16), Spectral (band 10), NBR, TXIT (band 5), TXIT (band 15), Spectral (band 33) and NDVI. Compared to the VNIR–SWIR bands typically used in burn severity mapping, the extra detailed MIR–TIR bands from MASTER were also expected to make a positive contribution to the understanding of the burn effects, taking advantage of their ability to record longer wavelength electromagnetic radiation. However, the variable selection results indicate that the VNIR–SWIR bands (1–25) remained vital to burn severity assessment, while the other bands (26–50) and associated texture and spectral indices did not have a high correlation with field-measure CBI as VNIR–SWIR did. Only band 33 from the MIR spectral range was selected. We further note that, among the three types of object-based variables (see Section 3.1), image-texture demonstrated higher likelihood to be more statistically relevant to CBI. In particular, three internal and one neighbourhood texture variables were selected by mRMR, suggesting that object-based spectral variability is a valuable indicator characterizing the differences in forest patches that suffered from fire-disease disturbances. Additionally, similar to the findings from previous research (De Santis and Chuvieco 2007; Fox, Maselli, and Carrega

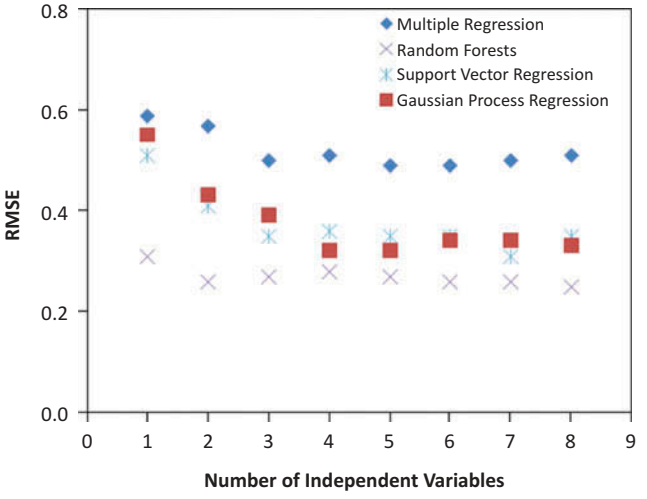

Figure 3. The performance (i.e., RMSEs) of the multiple regression, random forests, support vector regression and Gaussian process regression models using different combinations of variables selected by mRMR from top one to top eight.

2008), NBR and NDVI were found sensitive to the variation in burn severity, and NBR exhibited stronger capacity in the estimation of CBI.

The performance (i.e., RMSEs) of multiple regression, RF, SVM and GPR models showed similar trend lines applying different variable combinations selected by mRMR from top one to top eight (Figure 3). Specifically, if the number of variables was smaller than five, all the four types of models tended to be sensitive to the addition of more variables, with errors dramatically decreasing by approximately 17%, 16%, 31% and 42% for multiple regression, RF, SVM and GPR, respectively. In contrast, the error trend lines became relatively flat if more than five variables were applied, suggesting that the top four independent variables were already sufficient to our burn severity assessment, while the other variables may either have low correlations with CBI or only add redundancy to the existing model variables. Furthermore, the use of different variable combinations added higher variation to the results of SVR and GPR than to those of multiple regression and RF. One obvious reason is that the models are inherently different in structure. This could also be caused by the application of feature selection algorithm, where the 'best' variable combination selected by mRMR may not always be the best for other algorithms.

4.2. Comparison of model performance in burn severity assessment

The comparison of all the models' performance shows that machine learning outperformed multiple regression by 48%, 29% and 27% using RF, SVR and GPR, respectively (Figure 4). The model errors of multiple regression (using different variable combinations) ranged from 0.49 to 0.59, which were close to 20% of the most severe burn (i.e., CBI = 3), while machine learning proved to be more effective to reduce the burn severity estimation errors. Hence, our comparisons suggest that pre-fire disease outbreaks in a forest landscape could add high complexity to post-fire burn severity assessment, and conventional linear models are likely unable to capture the complex relationships between spectral measurements and burn severity. Using multiple regression is particularly problematic when numerous candidate predictors are available, for which variable selection is sensitive to random errors in observations. Our

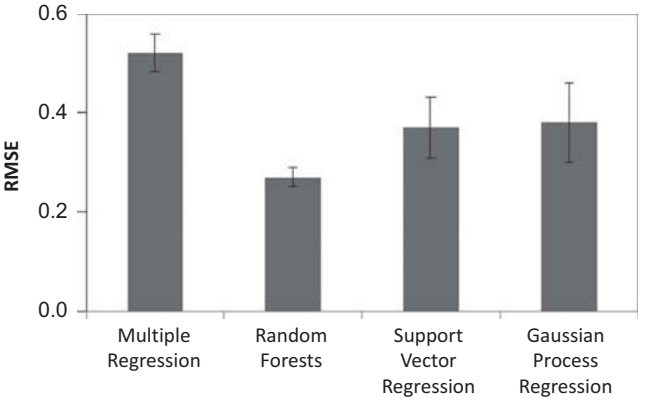

Figure 4. The comparison of the model average error (grey bar) and the error standard deviation (error bar) among the multiple regression, random forests, support vector regression and Gaussian process regression models.

analyses clearly demonstrate that machine learning often provides better alternative techniques because of their flexibility of modelling non-linear relationships based on limited observations. Of the three models tested here, SVR and GPR models had similar performances because they are exemplar-based kernel machines and we have used the RBF kernel for both of them. But we note that SVR often gives a sparse model that is fitted only from a subset of training samples, whereas GPR is a full model based on all the training samples. In our analyses, both SVR and GPR were outperformed by RF. The superiority of RF could probably be attributed to its ensemble-learning paradigm, that is, combining multiple weak learners into a strong learner. This model-averaging paradigm offers a theoretically appealing and practically effective inference framework to unravel complex remote sensing data sets, as demonstrated in both our results and earlier studies.

5. Conclusion

Three machine learning techniques, that is, GPR, RF and SVR, were introduced within a GEOBIA framework to assess burn severity in a forest landscape where an exotic disease, SOD, has caused pre-fire substantial tree mortality. Compared to the conventional multiple regression, RF, SVR and GPR reduced model errors by 48%, 29% and 27%, respectively, suggesting that a complex relationship exists between post-fire forest reflectance and the degree of burns in disease forests. Of the three tested machine-learning techniques, RF showed better performance in burn severity assessment and lower sensitivity to the application of different combinations of remote sensing variables. In addition to the widely used spectral index of NBR, we also found that image-texture representing spectral variability within and between neighbourhood forest patches was a valuable indicator characterizing the differences in forests that experienced fire-disease disturbances. Finally, we note that our model errors could be partly caused by the fact that the signals received by remote sensors are typically biased to the upper level of forest canopies, while the field-measured CBI values contain forest changes from all the strata. The inconsistency of spatial scale between field plot size and image resolution may have also caused errors. In our study, GEOBIA was applied to extract and analyse meaningful burned patches (average size of 0.8 ha) that simulated the actual burn effects in the field.

Acknowledgements

The authors thank Drs Ross Meentemeyer and David Rizzo for providing field and remote sensing data. We also appreciate the insightful comments from the editor and two anonymous reviewers.

Funding

This work was supported by North Carolina Space Grant and the University of North Carolina at Charlotte (UNCC) Faculty Research Grant and Seed Grant.

References

Bishop, C. 2006. *Pattern Recognition and Machine Learning*. New York: Springer.

Breiman, L. 2001. "Random Forests." *Machine Learning* 45: 5–32. doi:10.1023/A:1010933404324.

Chavez, P. 1996. "Image-Based Atmospheric Corrections – Revisited and Improved." *Photogrammetric Engineering and Remote Sensing* 62: 1025–1036.

Chen, G., and G. J. Hay. 2011. "A Support Vector Regression Approach to Estimate Forest Biophysical Parameters at the Object Level Using Airborne Lidar Transects and QuickBird Data." *Photogrammetric Engineering & Remote Sensing* 77: 733–741. doi:10.14358/PERS.77.7.733.

Chen, G., G. J. Hay, G. Castilla, B. St-Onge, and R. Powers. 2011. "A Multiscale Geographic Object-Based Image Analysis to Estimate Lidar-Measured Forest Canopy Height Using Quickbird Imagery." *International Journal of Geographical Information Science* 25: 877–893. doi:10.1080/13658816.2010.496729.

Cocke, A. E., P. Z. Fule, and J. E. Crouse. 2005. "Comparison of Burn Severity Assessments Using Differenced Normalized Burn Ratio and Ground Data." *International Journal of Wildland Fire* 14: 189–198. doi:10.1071/WF04010.

Cristianini, N., and J. Shawe-Taylor. 2000. *An Introduction to Support Vector Machines and Other Kernel-Based Learning Methods*. Cambridge: Cambridge University Press.

Dalponte, M., L. Bruzzone, and D. Gianelle. 2012. "Tree Species Classification in the Southern Alps Based on the Fusion of Very High Geometrical Resolution Multispectral/Hyperspectral Images and Lidar Data." *Remote Sensing of Environment* 123: 258–270. doi:10.1016/j.rse.2012.03.013.

De Santis, A., and E. Chuvieco. 2007. "Burn Severity Estimation from Remotely Sensed Data: Performance of Simulation versus Empirical Models." *Remote Sensing of Environment* 108: 422–435. doi:10.1016/j.rse.2006.11.022.

Fox, D. M., F. Maselli, and P. Carrega. 2008. "Using SPOT Images and Field Sampling to Map Burn Severity and Vegetation Factors Affecting Post Forest Fire Erosion Risk." *Catena* 75: 326–335. doi:10.1016/j.catena.2008.08.001.

Harris, S., S. Veraverbeke, and S. Hook. 2011. "Evaluating Spectral Indices for Assessing Fire Severity in Chaparral Ecosystems (Southern California) Using MODIS/ASTER (MASTER) Airborne Simulator Data." *Remote Sensing* 3: 2403–2419. doi:10.3390/rs3112403.

Harvey, B. J., D. C. Donato, W. H. Romme, and M. G. Turner. 2013. "Influence of Recent Bark Beetle Outbreak on Fire Severity and Postfire Tree Regeneration in Montane Douglas-Fir Forests." *Ecology* 94: 2475–2486. doi:10.1890/13-0188.1.

Hook, S. J., J. J. Myers, K. J. Thome, M. Fitzgerald, and A. B. Kahle. 2001. "The MODIS/ASTER Airborne Simulator (MASTER) – A New Instrument for Earth Science Studies." *Remote Sensing of Environment* 76: 93–102. doi:10.1016/S0034-4257(00)00195-4.

Hsu, C. W., C. C. Chang, and C. J. Lin. 2009. *A Practical Guide to Support Vector Classification*, 1–15. Technical Report. Taipei: Department of Computer Science, National Taiwan University.

Jenkins, M. J., E. Hebertson, W. Page, and C. A. Jorgensen. 2008. "Bark Beetles, Fuels, Fires and Implications for Forest Management in the Intermountain West." *Forest Ecology and Management* 254: 16–34. doi:10.1016/j.foreco.2007.09.045.

Kaufman, Y. J., and L. A. Remer. 1994. "Detection of Forests Using Mid-IR Reflectance: An Application for Aerosol Studies." *IEEE Transactions on Geoscience and Remote Sensing* 32: 672–683. doi:10.1109/36.297984.

Kealy, P. S., and S. J. Hook. 1993. "Separating Temperature and Emissivity in Thermal Infrared Multispectral Scanner Data: Implications for Recovering Land Surface Temperatures." *IEEE Transactions on Geoscience and Remote Sensing* 31: 1155–1164. doi:10.1109/36.317447.

Keith, H., B. G. Mackey, and D. B. Lindenmayer. 2009. "Re-Evaluation of Forest Biomass Carbon Stocks and Lessons from the World's Most Carbon-Dense Forests." *Proceedings of the National Academy Sciences of the United States of America* 106: 11635–11640. doi:10.1073/pnas.0901970106.

Kennedy, R. E., W. B. Cohen, and G. Takao. 1997. "Empirical Methods to Compensate for a View-Angle-Dependent Brightness Gradient in AVIRIS Imagery." *Remote Sensing of Environment* 62: 277–291. doi:10.1016/S0034-4257(97)00111-9.

Key, C., and N. Benson. 2006. "Landscape Assessment: Ground Measure of Severity; the Composite Burn Index, and Remote Sensing of Severity, the Normalized Burn Index." In *FIREMON: Fire Effects Monitoring and Inventory System*, edited by D. Lutes, R. Keane, J. Caratti, C. Key, N. Benson, S. Sutherland, and L. Gangi, 1–51. Fort Collins, CO: Rocky Mountains Research Station, USDA Forest Service.

Lentile, L. B., Z. A. Holden, A. M. S. Smith, M. J. Falkowski, A. T. Hudak, P. Morgan, S. A. Lewis, P. E. Gessler, and N. C. Benson. 2006. "Remote Sensing Techniques to Assess Active Fire Characteristics and Post-Fire Effects." *International Journal of Wildland Fire* 15: 319–345. doi:10.1071/WF05097.

Liaw, A., and M. Wiener. 2002. "Classification and Regression by Random Forest." *R News* 2/3: 18–22.

Malamud, B. D., J. D. A. Millington, and G. L. W. Perry. 2005. "Characterizing Wildfire Regimes in the United States." *Proceedings of the National Academy of Sciences of the United States of America* 102: 4694–4699. doi:10.1073/pnas.0500880102.

Meentemeyer, R. K., N. E. Rank, D. Shoemaker, C. Oneal, A. C. Wickland, K. M. Frangioso, and D. M. Rizzo. 2008. "Impact of Sudden Oak Death on Tree Mortality in the Big Sur Ecoregion of California." *Biological Invasions* 10: 1243–1255. doi:10.1007/s10530-007-9199-5.

Metz, M. R., K. M. Frangioso, R. K. Meentemeyer, and D. M. Rizzo. 2011. "Interacting Disturbances: Wildfire Severity Affected by Stage of Forest Disease Invasion." *Ecological Applications* 21: 313–320. doi:10.1890/10-0419.1.

Pasolli, L., F. Melgani, and E. Blanzieri. 2010. "Gaussian Process Regression for Estimating Chlorophyll Concentration in Subsurface Waters from Remote Sensing Data." *IEEE Geoscience and Remote Sensing Letters* 7: 464–468. doi:10.1109/LGRS.2009.2039191.

Peng, H., F. Long, and C. Ding. 2005. "Feature Selection Based on Mutual Information: Criteria of Max-Dependency, Max-Relevance, and Min-Redundancy." *IEEE Transactions on Pattern Analysis and Machine Intelligence* 27: 1226–1238. doi:10.1109/TPAMI.2005.159.

Rasmussen, C. E., and C. K. I. Williams. 2006. *Gaussian Processes for Machine Learning*. Cambridge, MA: The MIT Press.

Segal, M. R. 2003. "Machine Learning Benchmarks and Random Forest Regression." *eScholarship Repository*. University of California. http://repositories.cdlib.org/cbmb/bench_rf_regn

Teillet, P., B. Guindon, and D. Goodenough. 1982. "On the Slope-Aspect Correction of Multispectral Scanner Data." *Canadian Journal of Remote Sensing* 8: 84–106. doi:10.1080/07038992.1982.10855028.

Tucker, C. 1979. "Red and Photographic Infrared Linear Combinations for Monitoring Vegetation." *Remote Sensing of Environment* 8: 127–150. doi:10.1016/0034-4257(79)90013-0.

Vapnik, V. 1998. *Statistical Learning Theory*. New York: Wiley.

Veraverbeke, S., S. Hook, and G. Hulley. 2012. "An Alternative Spectral Index for Rapid Fire Severity Assessments." *Remote Sensing of Environment* 123: 72–80. doi:10.1016/j.rse.2012.02.025.

White, J. D., K. C. Ryan, C. C. Key, and S. W. Running. 1996. "Remote Sensing of Forest Fire Severity and Vegetation Recovery." *International Journal of Wildland Fire* 6: 125–136. doi:10.1071/WF9960125.

Zhao, K., S. Popescu, X. Meng, Y. Pang, and M. Agca. 2011. "Characterizing Forest Canopy Structure with Lidar Composite Metrics and Machine Learning." *Remote Sensing of Environment* 115: 1978–1996. doi:10.1016/j.rse.2011.04.001.

Zhao, K., S. Popescu, and X. Zhang. 2008. "Bayesian Learning with Gaussian Processes for Supervised Classification of Hyperspectral Data." *Photogrammetric Engineering & Remote Sensing* 74: 1223–1234. doi:10.14358/PERS.74.10.1223.